Available online at www.sciencedirect.com
SCIENCE DIRECT®
Journal of Sound and Vibration 278 (2004) 539–561
JOURNAL OF SOUND AND VIBRATION
www.elsevier.com/locate/jsvi

Energy dissipation of a friction damper

I. López[a,*], J.M. Busturia[b], H. Nijmeijer[a]

[a] *Dynamics and Control Group, Department of Mechanical Engineering, Eindhoven University of Technology, P.O. Box 513, 5600 MB Eindhoven, Netherlands*

[b] *GAMESA Corporación Tecnológica, S.A., Business Development Department, Zamudio Technology Park, Building 100, 48170 Zamudio, Bizkaia, Spain*

Received 21 March 2003; accepted 9 October 2003

Abstract

In this paper the energy dissipated through friction is analysed for a type of friction dampers used to reduce squeal noise from railway wheels. A one degree-of-freedom system is analytically studied. First the existence and stability of a periodic solution are demonstrated and then the energy dissipated per cycle is determined as a function of the system parameters. In this way the influence of the mass, natural frequency and internal damping of the friction damper on the energy dissipation is established. It is shown that increasing the mass and reducing the natural frequency and internal damping of the friction damper maximizes the dissipated energy.
© 2003 Elsevier Ltd. All rights reserved.

1. Introduction

Frictional forces arising from the relative motion of two contacting surfaces are a well-known source of energy dissipation. Sometimes this is an unwanted effect of the design, but it can also be intentionally used to increase the damping of a certain system in a simple and cost-effective way.

Some work has been done in the past to understand the behaviour of simple systems with Coulomb friction. Den Hartog [1] obtained closed-form analytical expressions for a single degree-of-freedom (DOF) system excited by a harmonic force. He showed both theoretically and experimentally that, depending on system parameters, the mass may continuously move or it may come to a stop during parts of each cycle. Years later Levitan [2] studied the forced oscillations of a mass-spring-damper system in which the support rather than the mass is excited. He used a Fourier series approximation for the Coulomb friction force that acts between the mass and the support. Hundal [3] obtained closed-form analytical expressions for a single DOF system with the

*Corresponding author. Fax: +31-40-246-1418.
E-mail address: i.lopez@tue.nl (I. López).

0022-460X/$ - see front matter © 2003 Elsevier Ltd. All rights reserved.
doi:10.1016/j.jsv.2003.10.051

Coulomb friction force acting between the mass and the ground. His work was limited to a maximum of two stops per cycle. Pratt and Williams [4] analyzed the relative motion of two masses with Coulomb friction contact. They used a combined analytical-numerical approach to obtain the response of the system for arbitrary values of the friction force, excitation frequency and natural frequency of the bodies. They showed that under certain conditions multiple lock-ups per cycle are possible and that for frequency ratios ω_0/ω_n (excitation frequency versus natural frequency) below 0.5 no continuous sliding motion is possible. Their results were limited to two blocks with the same mass and spring stiffness and support motion of the same amplitude and frequency.

The aim of the research in the publications described above is to analyse whether the motion is continuous or if several stops per cycle occur and also to determine the influence of the system parameters on the response amplitude. In the majority of these publications, no attention has been paid to the analysis of the influence of the system parameters on the energy dissipated by friction and no work has been done to investigate which conditions maximize the energy dissipation. Beards and Williams [5] analyzed the damping due to rotational slip in structural joints. They studied a two DOF system and concluded, from both analytical and experimental results, that, as the friction force increases the response amplitude goes through a minimum. Later Beards and Woowat [6] carried out an experimental study of a steel frame where the joint clamping forces could be varied. They found that an optimum clamping force exists that minimizes the frame response but they did not investigate the dependence of the optimum on the system parameters. More recently, in his review of friction-induced vibration Ibrahim [7] compares the energy dissipated by friction to the energy dissipated by a viscous damper showing that the former is larger than the latter.

Another review on friction related phenomena has been published by Akay [8]. In this publication the use of ring dampers in order to reduce the vibration of the rotor in disk-brakes is mentioned. Ring dampers reduce vibrations by means of friction between the ring and the rotor. Very significant reductions of the bending vibrations of the rotor are achieved. A similar concept was used by López [9] to reduce squeal noise in railway wheels. A ring damper was developed in [9] that greatly reduces the bending vibrations of the wheel.

In the current paper an analytical study for a better understanding and optimization of the behaviour of ring dampers is presented. This study was originally intended for ring dampers for railway wheels but the same conclusions could be applied to ring dampers for other types of wheels or disks undergoing high axial (bending) vibrations. During squeal one or two bending vibration modes of the wheel are predominant in the response [9–12]. If the wheel is vibrating in a given mode, it can be assumed that the ring will follow the same pattern and the system can be simplified to a mode to mode interaction, thus two DOFs [9]. This is an oversimplification of the wheel/ring interaction, but it allows studying the qualitative influence of the main parameters of the ring damper.

In order to determine the influence of several parameters on the amount of energy dissipated by friction, one and two DOF systems will be analyzed. Those systems are very simple models of the full wheel/ring interaction and their aim is to show the influence of the friction force and ring mass, natural frequencies and damping on the dissipated energy.

Many different models are proposed for the mathematical description of dry-friction which mostly differ in the way the stick phase is modelled [13]. The aim of this work is to gain insight on

the behaviour of a friction damper through analytical models and produce simple rules to maximize the energy dissipation. The classical Coulomb's friction law has been chosen for simplicity, since more complex models would make an analytical approach intractable. In the following analysis the simplest form of Coulomb's friction, with equal static and dynamic friction coefficients, is used (Fig. 1(a)). In Appendix A the possibility of having different static and dynamic friction coefficients is studied (Fig. 1(b)). It is shown that for the situation under study (steel–steel contact) the same conclusions can be derived with respect to the optimization of the system parameters for maximum energy dissipation.

In Section 2 a mass sliding on a moving base is studied and the existence and stability of periodic steady state oscillations is investigated. It is shown that, regardless of the value of the friction force, a periodic stationary motion exists and that this motion is stable.

In Section 3 the energy dissipated through friction in the steady state is determined for a mass sliding on a moving base. This case applies to a situation in which the wheel is massive compared to the ring and vibrates undisturbed by the latter. The natural frequencies of the ring are well below the oscillation frequency of the wheel; thus, the response of the former is determined by its mass. The results are also extended to a block sliding on another block driven by a harmonic external force. This example represents a case in which wheel and ring can have masses of the same order of magnitude, but still the oscillation frequency of the external force must be well above the natural frequencies of both. With this example the effect of the mass ratio of the structures on the energy dissipated by friction will be shown.

The analysis of Section 3 is extended in Section 4 to a mass attached to a fixed support through a spring and a damper. In this case the influence of the ratio of the oscillation frequency to the natural frequency of the spring-mass system and of the damping ratio on the dissipated energy is studied. With this example, the effect of the magnitude of the ring natural frequencies relative to the vibration frequency of the wheel and of increasing the internal damping of the ring is shown.

In most of the above examples the wheel is taken as an ideal velocity source, with a fixed vibration frequency. A single ring natural frequency is considered, which is equivalent to having a mode to mode interaction. Despite these simplifications, the models proposed give sufficient insight into the behaviour of ring dampers [14,15].

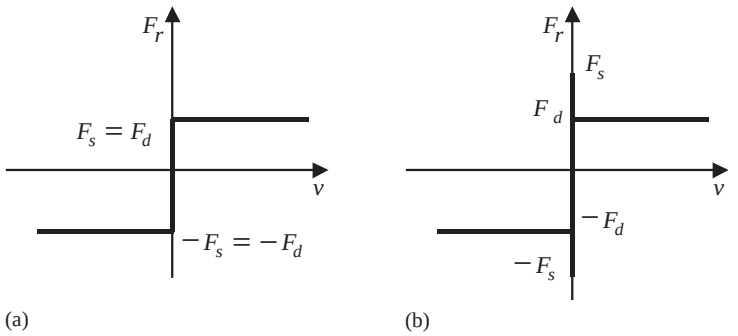

Fig. 1. Coulomb friction model with (a) $F_s = F_d$ and (b) $F_s \neq F_d$.

2. Stationary periodic behaviour and stability

2.1. Existence of a stationary periodic solution

Before proceeding to derive an expression for the energy dissipated through friction in the systems shown in Fig. 2, the existence of a steady state periodic behaviour will be checked.

In order to keep the equations simple, the existence of a stationary periodic motion will be analysed for the simplest case of the mass sliding on a moving base shown in Fig. 2(a). A block of mass m is loaded, with a normal force N, against the surface of the base. The surface moves with a sinusoidal displacement $x_0(t) = X_0 \sin \omega_0 t$ and the block follows with a displacement $x_2(t)$. The base motion is transmitted to the block through the friction force. There are two possible motions for the block: stick (velocity of block equals velocity of base) or slip (velocity of block different from velocity of base).

In the stick situation the velocity and acceleration of the block are

$$\left.\begin{aligned} \dot{x}_2(t) &= \dot{x}_0(t) = \omega_0 X_0 \cos \omega_0 t \\ \ddot{x}_2(t) &= \ddot{x}_0(t) = -\omega_0^2 X_0 \sin \omega_0 t \end{aligned}\right\} \; t_0 \leqslant t \leqslant t_1. \tag{1}$$

Eq. (1) will hold until the acceleration of the block equals the limiting value given by the friction force:

$$\sin \omega_0 t_1 = \pm \frac{F_r}{\omega_0^2 X_0 m} = \pm f_r. \tag{2}$$

In this expression a normalized friction force parameter, f_r, has been defined. The positive or negative sign in (2) corresponds to a negative or positive acceleration of the base. From (2) it becomes clear that time t_1 will only exist if $|f_r| < 1$. This gives an upper bound for the friction force above which no slip occurs. For $|f_r| \geqslant 1$ the block will permanently move with the same displacement, velocity and acceleration as the base.

In the slip phase the velocity and acceleration of the block are:

$$\left.\begin{aligned} \dot{x}_2(t) &= \omega_0 X_0 [\mp \omega_0 f_r (t - t_1) + \cos \omega_0 t_1] \\ \ddot{x}_2(t) &= \mp f_r \omega_0^2 X_0 \end{aligned}\right\} \; t_1 \leqslant t \leqslant t_2. \tag{3}$$

The negative or positive sign in (3) corresponds to a negative or positive acceleration of the base. Eqs. (3) will hold until the velocities of the block and the base are equal, $\dot{x}_2(t_2) = \dot{x}_0(t_2)$. From this condition the following equation can be obtained:

$$\omega_0 f_r (t_2 - t_1) = \pm (\cos \omega_0 t_1 - \cos \omega_0 t_2). \tag{4}$$

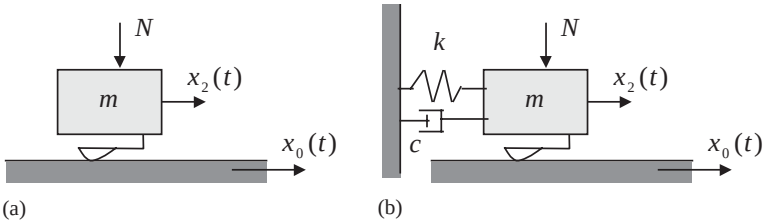

Fig. 2. 1 DOF systems. (a) mass on a moving base and (b) spring-mass-damper.

The positive or negative sign in (4) corresponds to a negative or positive acceleration of the base. The above expression can be used to numerically calculate t_2 the knowledge of t_1, the normalized friction force and the frequency of the base motion.

If t_1 and t_2 are the limits of the slip phase for the half-cycle of negative acceleration of the base and t_3 and t_4 are the corresponding limits for the half-cycle of positive acceleration of the base, as shown in Fig. 3, it can be concluded from (1) and (3) that

$$t_3 = t_1 + \frac{\pi}{\omega_0}, \quad t_4 = t_2 + \frac{\pi}{\omega_0}. \tag{5}$$

Since $t_2 < t_3$, it is also true that $t_4 < t_1 + 2\pi/\omega_0$, which means that at t_4 the block and the base will move together again until the cycle is completed at time $t_5 = t_1 + 2\pi/\omega_0$. Therefore, the stick-slip motion of the block is periodic with frequency ω_0.

For low values of f_r the block will continuously slide on the base. The limit situation when the block enters the sliding regime corresponds to a friction force such that at time t_2 the acceleration of the base surface is equal to the limiting value given by the friction force and the mass of the block:

$$\sin \omega_0 t_2 = -f_r. \tag{6}$$

In this particular situation it follows from (5) and (6) that

$$t_2 = t_3 = t_1 + \frac{\pi}{\omega_0} \quad \text{and} \quad t_4 = t_1 + \frac{2\pi}{\omega_0}. \tag{7}$$

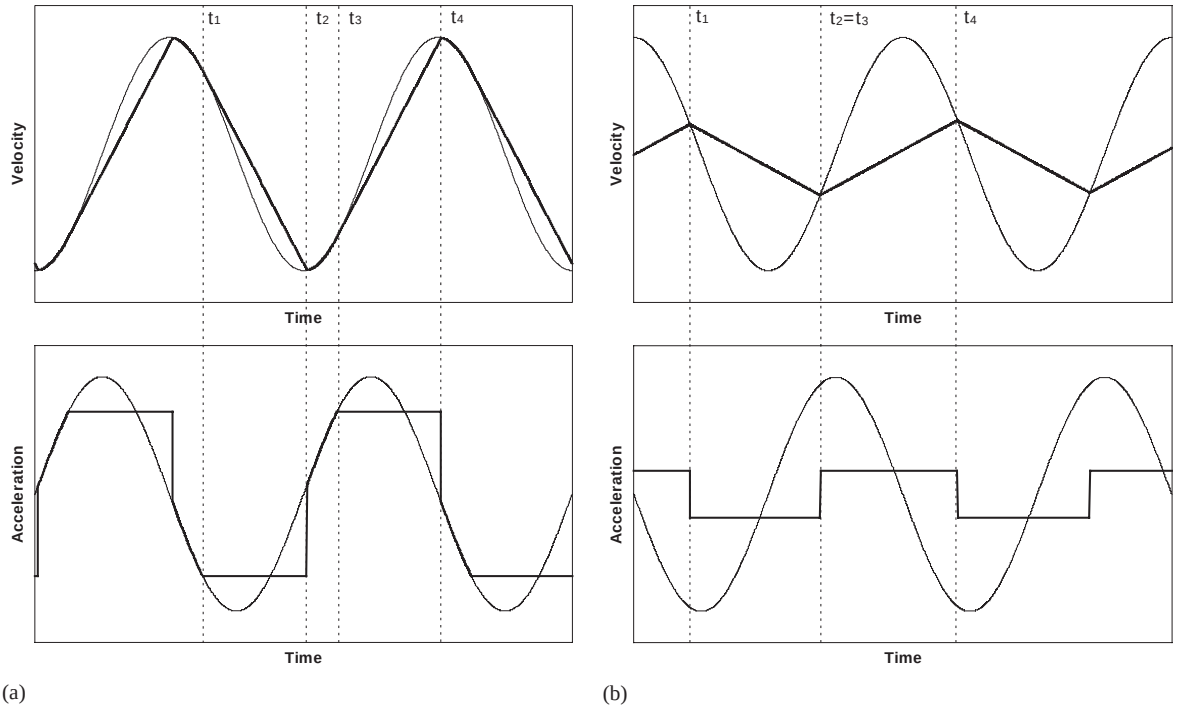

Fig. 3. Velocity (top) and acceleration (bottom) of the block (thick line) and the base (thin line). (a) $f_r = 0.7$ and (b) $f_r = 0.2$.

The block's motion is still periodic. Taking into account Eqs. (2) and (7), an expression for the threshold normalized friction force can be derived from (4):

$$f_r|_{threshold} = \sqrt{\frac{1}{1+\frac{\pi^2}{4}}} \approx 0.5370. \tag{8}$$

It can be concluded that $f_r|_{threshold}$ is constant and the threshold friction force for the onset of permanent sliding is linearly related to the block mass and base acceleration amplitude. For normalized friction forces smaller than the threshold value given by (8) the block will permanently slide.

In the continuous sliding situation it can be numerically shown that, although in the first cycles there is no periodicity relationship between the time instants t_1, t_2 and t_4, the relationships given in (7) hold after a few cycles of motion. However, t_1 no longer complies with Eq. (2), because at the steady state there is no time instant at which, the relative velocity being zero, the accelerations of block and base coincide. Now t_1 is any time at which the velocity of the block equals the velocity of the base; i.e. the time at which the friction force acting on the mass changes sign.

The existence of a periodic solution can be proved by choosing an initial value for t_1 and then solving Eq. (4) with alternating signs for several cycles of the motion. In this way the time instants where the sign of the friction force changes can be determined (that is, the positions of the local maxima and minima of the velocity of the block). In Fig. 4 the angle, $\omega_0\Delta t$, between a maximum and a minimum and between two consecutive maxima divided π, and 2π respectively is given. It is clear that after a few cycles the angle between two consecutive maxima tends to 2π and each of the half cycles has length π.

Now a new expression for the normalized friction force in terms of time t_1 can be found from (4) and (7):

$$f_r = \frac{2}{\pi}\cos\omega_0 t_1. \tag{9}$$

The same procedure can be followed for the spring-mass-damper system shown in Fig. 2(b) and equations similar to (2) and (4) can be derived. But it becomes cumbersome to trace the response of the system analytically. If the damping is set to zero, Deimling [16,17] has shown that a periodic

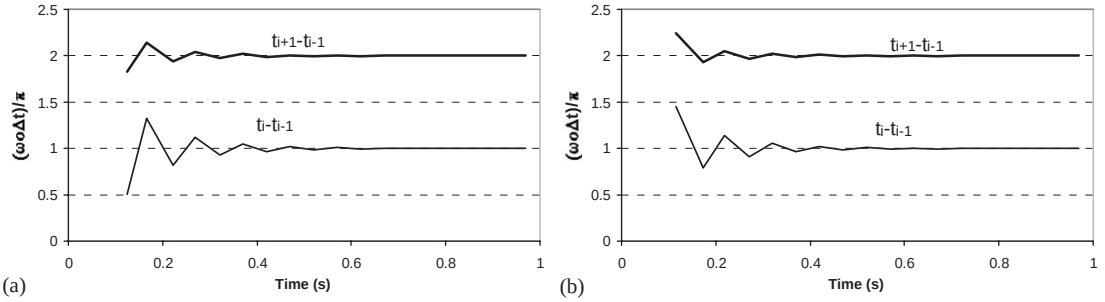

Fig. 4. Non-dimensional length of a half (lower) and full (upper) cycle, for $f_r = 0.2$ and 2 arbitrary initial values of t_1.

solution exists for such a system. The periodic solution is also found if the dynamic equations of the system are numerically integrated.

The present analysis is limited to values of the natural frequency of the spring-mass-damper below the oscillation frequency of the base, $\omega_n/\omega_0 < 1$, since wheel/ring interaction occurs mainly between modes with an equal number of nodal diameters [18], which means that the natural frequencies of the ring (block) will be lower than the natural frequencies of the wheel (base). In their work with two friction-coupled oscillators Pratt and Williams [4] found that for $\omega_n/\omega_0 > 2$ continuous sliding motion is not possible and more than two lock-ups per cycle can occur. For $\omega_n/\omega_0 < 1$, however, two types of motion have been found: permanent slip or stick-slip motion with two lock-ups per cycle.

2.2. Stability of the periodic solution

In the previous subsection it has been shown that a periodic stationary solution exists. The goal of this subsection is to prove that this periodic stationary solution is also a stable solution. To this end the Floquet multipliers for the periodic solutions of the systems in Fig. 2 will be used. These systems are non-linear non-autonomous systems and the differential equation that represents them is

$$\dot{\mathbf{x}}(t) = \mathbf{f}(t, \mathbf{x}(t)) \quad \text{with } \mathbf{x}(t)^{\mathrm{T}} = [x(t)\ \dot{x}(t)]. \tag{10}$$

Starting from Eq. (10) and linearizing around a periodic solution an expression that relates a perturbation at a given time t_0 to the perturbation at another time t can be obtained:

$$\Delta\mathbf{x}(t) = \mathbf{\Phi}(t, t_0)\, \Delta\mathbf{x}(t_0). \tag{11}$$

$\mathbf{\Phi}(t, t_0)$ is the fundamental solution matrix and its value after one period of the motion, $\mathbf{\Phi_T} = \mathbf{\Phi}(t_0 + T, t_0)$ is called the monodromy matrix. The Floquet multipliers for a given periodic solution of Eq. (10) are the eigenvalues of the monodromy matrix. The solution is locally stable if the norms of the Floquet multipliers are all smaller than 1 [13,19].

For the system under study the above statements must be handled with care. This system is a non-smooth system and the monodromy matrix might be undetermined if the initial time t_0 corresponds to the transition from slip to stick or to the stick phase. In the following analysis, t_0 is a time instant at which the block is sliding.

The right hand side of (10) is discontinuous, since a different expression will hold depending on if the block sticks to the base or if it slips. This has important consequences for the derivation of the monodromy matrix. As the block changes from slip to stick, or from stick to slip, a jump might occur. This jump is introduced in the monodromy matrix through saltation matrices [13]. The details over the derivation of the monodromy matrix and Floquet multipliers are given in Appendix B. In the following the main results will be discussed.

The stability of the stick-slip periodic solution will be proved first. The monodromy matrix for the stick-slip periodic solution of the systems in Fig. 2 can be written as follows:

$$\mathbf{\Phi_T} = \mathbf{\Phi}(\Delta t_5)\mathbf{S_2}\,\mathbf{\Phi}^S(\Delta t_4)\mathbf{S_1}\mathbf{\Phi}(\Delta t_3)\mathbf{S_2}\mathbf{\Phi}^S(\Delta t_2)\mathbf{S_1}\mathbf{\Phi}(\Delta t_1), \tag{12}$$

where $\mathbf{\Phi}(\Delta t_1)$ are the fundamental solution matrices when the block is sliding, $\mathbf{\Phi}^S(\Delta t_i)$ are the fundamental solution matrices for the time intervals where the block sticks to the base and $\mathbf{S}_i$ are

saltation matrices. The time instants when the block changes from slip to stick and from stick to slip can be determined from Eqs. (2), (4) and (5) for the system in Fig. 2(a) and from analogous expression for the system in Fig. 2(b). In both cases, it is shown in Appendix B that the saltation matrices are

$$\mathbf{S}_1 = \begin{bmatrix} 1 & 0 \\ 0 & 0 \end{bmatrix}, \quad \mathbf{S}_2 = \mathbf{I} = \begin{bmatrix} 1 & 0 \\ 0 & 1 \end{bmatrix} \tag{13}$$

$\mathbf{S}_1$ is the saltation matrix from slip to stick, and $\mathbf{S}_2$ is the saltation matrix from stick to slip. In the latter case, the transition from stick to slip is smooth and there is no jump, because the friction law chosen is such that the dynamic and static friction coefficients are the same (Fig. 1(a)).

An important consequence of Eq. (13) is that $\mathbf{S}_1$ is singular, which means that the monodromy matrix is also singular and, therefore, one of the Floquet multipliers is always equal to zero. The physical meaning of this is that as the solution enters the stick phase, knowledge of the initial velocity is lost and solutions entering the stick phase with different velocities will all leave the stick phase with the same velocity.

For the mass on a moving base from Fig. 2(a) an analytical expression for $\mathbf{\Phi_T}$ can be derived and the second Floquet multiplier can be determined:

$$\text{Stick-slip } (k = 0, c = 0)\text{: } \mathbf{\Phi_T} = \begin{bmatrix} 1 & \Delta t_1 \\ 0 & 0 \end{bmatrix},$$
$$\text{Floquet multipliers: } \quad \lambda_1 = 1, \lambda_2 = 0. \tag{14}$$

As could be expected, the second Floquet multiplier is 1. If the mass, which is oscillating at a given position on the base, is taken to a different position, it will go on oscillating in that position. All positions on the base are stable positions for that periodic solution. This result is further discussed in Appendix B.

It can easily be seen that the situation changes if a spring is attached to the block and to a fixed reference. In that case, it is shown in Appendix B that $\lambda_1 = \cos^2\theta < 1$. If a damper is added, it becomes cumbersome to derive an analytical expression for λ_1, but computer calculations show that it is smaller than 1. Therefore, the stick-slip periodic solution is also stable for the spring-mass-damper system.

For the continuous sliding situation, the monodromy matrix has the following form:

$$\mathbf{\Phi_T} = \mathbf{\Phi}(\Delta t_3)\mathbf{S}\mathbf{\Phi}(\Delta t_2)\mathbf{S}\mathbf{\Phi}(\Delta t_1), \tag{15}$$

where $\mathbf{\Phi}(\Delta t_i)$ are the fundamental solution matrices when the block is sliding and $\mathbf{S}$ is the saltation matrix for the transitions from positive to negative and negative to positive acceleration of the block. The time instants when the acceleration of the block changes sign can be determined from (7) and (9) for the mass on a moving base and from analogous expressions if a spring and a damper are attached to the mass. As shown in Appendix B, the saltation matrix has the form given below:

$$\mathbf{S} = \begin{bmatrix} 1 & 0 \\ 0 & \alpha \end{bmatrix} \quad \text{with } 0 < \alpha < 1 \quad \Rightarrow \quad 0 < \det(\mathbf{S}) < 1. \tag{16}$$

For the mass on a moving base from Fig. 2(a) an analytical expression for $\mathbf{\Phi_T}$ can be derived and the Floquet multipliers can be determined:

$$\text{Sliding } (k=0, c=0): \quad \mathbf{\Phi_T} = \begin{bmatrix} 1 & \Delta t_1 + \alpha \Delta t_2 + \alpha^2 \Delta t_3 \\ 0 & \alpha^2 \end{bmatrix},$$
$$\text{Floquet multipliers:} \quad \lambda_1 = 1,\ \lambda_2 = \alpha^2 < 1. \tag{17}$$

For the same reason explained before one of the Floquet multipliers is 1 and the other one is smaller than 1, which means that the harmonic continuous sliding solution is stable when $\omega_n/\omega_0 \to 0$. The same conclusion can be reached by looking at the determinant of the monodromy matrix:

$$\det(\mathbf{\Phi_T}) = \det(\mathbf{\Phi}(\Delta t_3))\det(\mathbf{S})\det(\mathbf{\Phi}(\Delta t_2))\det(\mathbf{S})\det(\mathbf{\Phi}(\Delta t_1))$$
$$\text{with } \det(\mathbf{\Phi}(\Delta t_i)) = 1 \quad \text{and} \quad 0 < \det(\mathbf{S}) < 1$$
$$\Rightarrow \quad \det(\mathbf{\Phi_T}) = \det(\mathbf{S})\ \det(\mathbf{S}) < 1, \tag{18}$$

Since it can be said a priori that one of the Floquet multipliers is 1, it can be concluded that the other one has to be smaller than 1. The above derivation is also valid when a spring and a damper are attached to the block, because Eq. (16) has been derived for an arbitrary value of $\omega_n/\omega_0 < 1$ and damping. But in this case, the value of the Floquet multipliers cannot be established a priori and that $\det(\mathbf{\Phi_T}) = \lambda_1\lambda_2 < 1$ does not guarantee stability, i.e. $|\lambda_1| < 1, |\lambda_2| < 1$.

However, computer calculations show that the Floquet multipliers are smaller than one for the considered values of $\omega_n/\omega_0 < 1$ with and without damping. Results for several different damping values are given in Appendix B. Therefore, it can be concluded that the continuous sliding periodic solution is also stable.

3. Energy dissipation: mass on a moving base

In the previous section it has been shown that, depending on the value of the friction force, two stable stationary periodic solutions exist for the systems in Fig. 2. Therefore the groundwork has been laid for the calculation of the energy dissipation at the friction interface and of its dependence on the friction force and the mass of the block.

The energy dissipated per cycle can be calculated as the integral of the product of the dissipating force times the relative velocity between block and base. This relative velocity is only non-zero at time intervals $[t_1, t_2]$ and $[t_3, t_4]$. Taking into account the periodicity relationships between time instants t_1, t_3 and t_2, t_4 given in Eq. (7), the dissipated energy for an arbitrary cycle in the steady state can be written as follows:

$$E_d = 2 \int_{t_1}^{t_2} -F_r(\dot{x}_0(t) - \dot{x}_2(t))\, \mathrm{d}t \tag{19}$$

Substituting Eq. (3) in (19), the following expression for the energy dissipated per cycle can be derived:

$$e_d = 2\omega_0 f_r(t_2 - t_1)\left[\frac{(\sin\omega_0 t_1 - \sin\omega_0 t_2)}{\omega_0(t_2 - t_1)} + \cos\omega_0 t_1 - \frac{\omega_0 f_r}{2}(t_2 - t_1)\right]. \tag{20}$$

In this equation the energy has been normalized to be: $e_d = E_d/m\omega_0^2 X_0^2$.

The above expression is valid for both the stick-slip and the continuous sliding situations, that is for all values of the friction force in the range $0 < f_r < 1$. In the stick-slip region equations (2), (4) and (20) can be used to compute the energy dissipated per cycle from known values of the normalized friction force and the frequency of the base motion. For the continuous sliding equations (7) and (9) can be substituted in (20) to obtain expressions of the energy dissipation in terms of t_1 and of the normalized friction force for continuous sliding:

$$e_d = \frac{4}{\pi}\sin 2\omega_0 t_1, \tag{21}$$

$$e_d = 4f_r\sqrt{1 - \frac{\pi^2 f_r^2}{4}}. \tag{22}$$

In Fig. 5 a graph of the normalized energy versus the normalized friction force, in the range $0 < f_r < 1$, is plotted. The curve has been computed using (20) and (22). The part of the curve corresponding to continuous sliding can be obtained analytically from (22), but the energy dissipation for the stick-slip case has to be calculated numerically from (2), (4) and (20), since no closed-form expressions for time instant t_2 can be derived in this case.

The thick dashed line corresponds to the limit situation. To the right of this line stick-slip motion will occur and, to the left, the block will permanently slip once sliding has occurred. The dissipated energy drops to zero when the friction force is zero and when the friction force is high enough to keep block and base together and equals the base acceleration amplitude times the mass of the block.

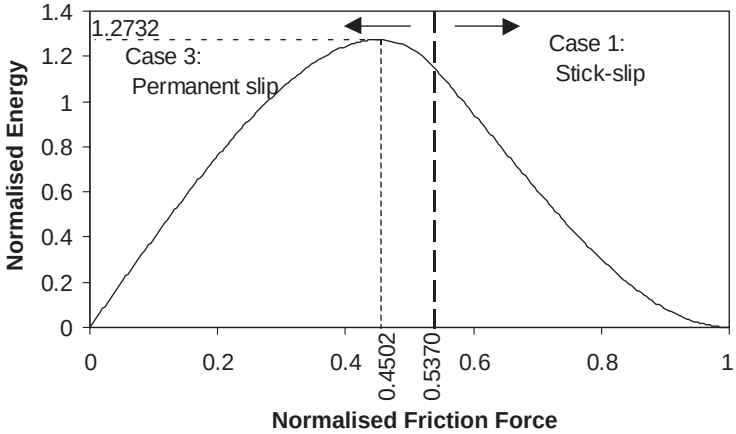

Fig. 5. Dissipated energy/friction force in the range $0 < f_r < 1$.

From Fig. 5 it is clear that the maximum energy dissipation is achieved in the continuous sliding region and it can be easily seen, from (21), that this maximum occurs when $\omega_0 t_1 = \pi/4$. Substituting this in (9), the value of the optimum normalized friction force can be calculated:

$$f_r|_{\max} = \frac{\sqrt{2}}{\pi} = 0.4502. \tag{23}$$

The optimum normalized friction force is a constant and it is smaller than the threshold force, as could be expected from Fig. 5. The maximum normalized energy dissipation will be

$$e_d|_{\max} = \frac{4}{\pi} = 1.2732. \tag{24}$$

Eq. (24) shows that the value of the maximum achievable energy dissipation is independent of the friction force and depends only on the block mass and the amplitude of the vibration velocity of the base.

The analysis of this simple model has helped to clarify two aspects of frictional interaction as a source of energy dissipation: the existence of an optimum friction force value and the positive influence of the block mass on the dissipated energy. The values of the optimum friction force and of the corresponding maximum energy dissipation have been analytically determined.

In their work with two base excited mass-spring systems Pratt and Williams [4] calculated the dissipated energy numerically and plotted it as function of a normalized friction parameter, showing there was a maximum. But no closed form expression for the optimum friction force and maximum dissipated energy were given.

If the mass of the base is taken into account and a system such as that given in Fig. 6 is considered, the same expressions hold for the threshold and optimum friction force and for the maximum energy dissipation provided that the normalized parameters are redefined as follows: $f_r = F_r(M+m)/Fm$, $e_d = E_d[\omega_0^2 M(M+m)/mF^2]$.

From (24), the maximum energy dissipation can be obtained:

$$E_d|_{\max} = \frac{4}{\pi}\frac{F^2}{\omega_0^2 M}\frac{1}{\left(1+\dfrac{M}{m}\right)}. \tag{25}$$

The maximum dissipated energy increases as the ratio of the mass of block 2 to the mass of block 1 increases. For $m \ll M$ the maximum energy dissipation is linearly related to m, which is the same result obtained before. It can also be concluded that as the ratio m/M increases the benefit of increasing the mass of the block becomes smaller.

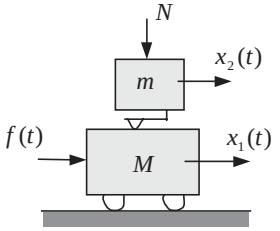

Fig. 6. Two masses with external force excitation.

4. Energy dissipation: spring-mass-damper system on a moving base

This case can be considered as an extension of the example in Section 3, in which a spring of stiffness k and a viscous damper of damping constant c are attached to the block of mass m, as shown in Fig. 2(b). The natural frequency of the spring-mass system is $\omega_n = \sqrt{k/m}$, the damping ratio is defined as $\xi = c/2m\omega_n$ and the damped natural frequency is $\omega_d = \omega_n\sqrt{1-\xi^2}$.

After the system is in motion for some time, a steady state will be reached that satisfies the following conditions: the frequency of the relative motion will be equal to the frequency of the base motion and the downward half-cycle of motion will follow the same law as the upward half-cycle.

Now consider the half-cycle in which the relative velocity, and thus the friction force, is negative. t_1 is the time at which the relative velocity changes from being zero (stick-slip) or positive (continuous sliding) to being negative and t_2 is the time at which the relative velocity is zero again. In both cases the velocity of the block at times t_1 and t_2 is equal to the velocity of the base. The displacement of the block in the time interval $[t_1, t_2]$ can be computed as the sum of the response of the spring-mass system to the initial conditions and the response to the friction force, F_r. In the following equation $\tilde{t} = t - t_1$:

$$x_2(t) = \mathrm{e}^{-\xi\omega_n\tilde{t}}\left[x_2(t_1)\left(\cos\omega_d\tilde{t} + \frac{\xi\sin\omega_d\tilde{t}}{\sqrt{1-\xi^2}}\right) + \frac{\dot{x}_2(t_1)}{\omega_d}\sin\omega_d\tilde{t}\right] - \frac{F_r}{k}\left[1 - \mathrm{e}^{-\xi\omega_n\tilde{t}}\left(\cos\omega_d\tilde{t} + \frac{\xi\sin\omega_d\tilde{t}}{\sqrt{1-\xi^2}}\right)\right]. \tag{26}$$

The boundary conditions that must be fulfilled in both the stick-slip and the continuous sliding regime are

$$\dot{x}_2(t_1) = \dot{x}_0(t_1), \tag{27}$$

$$\dot{x}_2(t_2) = \dot{x}_0(t_2), \tag{28}$$

$$x_0(t_1) - x_2(t_1) = -(x_0(t_2) - x_2(t_2)). \tag{29}$$

The fourth boundary condition that holds only in the stick-slip case:

$$\ddot{x}_2(t_1) = \ddot{x}_0(t_1), \tag{30}$$

And for continuous sliding the fourth boundary condition is

$$t_2 = t_1 + \pi/\omega_0. \tag{31}$$

In these equations four unknowns must be determined: t_1, t_2, $x_2(t_1)$ and $\dot{x}_2(t_1)$. For the stick-slip regime, Eqs. (27)–(30) have to be solved numerically to compute t_1, t_2 and $x_2(t_1)$ from given values of base vibration amplitude, frequency, spring stiffness, damping ratio, block mass and friction force.

For the continuous sliding case, t_2 can be directly computed from (31) and Eqs. (27)–(29) can be simplified to obtain a closed-form expression for the normalized friction force as a

function of t_1:

$$f_r = B\left(\frac{\omega_n}{\omega_0}, \xi\right)\cos\omega_0 t_1. \tag{32}$$

In (32), f_r is the same normalized friction parameter defined in (2) and B is given in Appendix B. If $\xi \to 0$ and $\omega_n/\omega_0 \to 0$ Eq. (32) equals (9). The energy dissipated per cycle can be obtained from (19).

$$e_d = 2f_r\left\{\sin\omega_0 t_1 - \sin\omega_0 t_2 + \mathrm{e}^{-\xi\omega_n t_{21}}\left(\frac{\omega_0}{\omega_d}\cos\omega_0 t_1 \sin\omega_d t_{21}\right)\right.$$
$$\left. - \left(\frac{x_2(t_1)}{X_0} + \frac{f_r\omega_0^2}{\omega_n^2}\right)\left[1 - \mathrm{e}^{-\xi\omega_n t_{21}}\left(\cos\omega_d t_{21} + \frac{\xi}{\sqrt{1-\xi^2}}\sin\omega_d t_{21}\right)\right]\right\}, \tag{33}$$

where $t_{21} = t_2 - t_1$. The same normalization factor defined in Section 3 has been used to define the normalized energy dissipation given in (33). This expression holds in every case, no matter whether the block slips continuously or stick-slip motion occurs. In the continuous sliding regime, Eqs. (27)–(29) and (31) can be used to simplify this equation and derive an expression for the normalized energy dissipation:

$$e_d = \frac{\omega_d}{\omega_0}\frac{\mathrm{e}^{\xi\,\omega_n\pi/\omega_0} + \mathrm{e}^{-\xi\,\omega_n\pi/\omega_0} + 2\cos\dfrac{\omega_d\pi}{\omega_0}}{\sin\dfrac{\omega_d\pi}{\omega_0}}$$
$$\times\left(\sin 2\omega_0 t_1 + \frac{\omega_0}{\omega_n}\sqrt{1-\xi^2}\,\frac{\mathrm{e}^{-\xi\omega_n\pi/\omega_0} - \mathrm{e}^{\xi\omega_n\pi/\omega_0} + 2\dfrac{\xi}{\sqrt{1-\xi^2}}\sin\dfrac{\omega_d\pi}{\omega_0}}{\sin\dfrac{\omega_d\pi}{\omega_0}}\cos^2\omega_0 t_1\right). \tag{34}$$

It can be shown that, if $\xi \to 0$ and $\omega_n/\omega_0 \to 0$, this expression equals Eq. (21). If the first derivative of Eq. (34) with respect to $\omega_0 t_1$ is equated to zero an expression for $\omega_0 t_1|_{\max}$ can be obtained:

$$\tan 2\omega_0 t_1|_{\max} = 2\frac{\omega_n}{\omega_0\sqrt{1-\xi^2}}\frac{\sin\dfrac{\omega_d\pi}{\omega_0}}{\mathrm{e}^{-\xi\,\omega_n\pi/\omega_0} - \mathrm{e}^{\xi\,\omega_n\pi/\omega_0} + 2\dfrac{\xi}{\sqrt{1-\xi^2}}\sin\dfrac{\omega_d\pi}{\omega_0}}. \tag{35}$$

Eq. (35) gives the value of $\omega_0 t_1$ for which the normalized energy expression given by (34) is maximized. When $\xi \to 0$ and $\omega_n/\omega_0 < 1$, $\omega_0 t_1|_{\max}$ tends to 45°. If the maximum energy dissipation occurs in the continuous sliding motion range, substitution of Eq. (35) into (34) gives the value of the maximum dissipated energy. For the case of $\xi \to 0$ simple closed form expressions can be obtained for the optimal normalized friction and the maximum dissipated energy as a function of

the frequency ratio ω_n/ω_0:

$$f_r|_{\max} = \frac{\omega_n}{\omega_0}\frac{1+\cos(\omega_n\pi/\omega_0)}{\sqrt{2}\sin(\omega_n\pi/\omega_0)}, \tag{36}$$

$$e_d|_{\max} = 2\frac{\omega_n}{\omega_0}\frac{1+\cos(\omega_n\pi/\omega_0)}{\sin(\omega_n\pi/\omega_0)}. \tag{37}$$

When $\omega_n/\omega_0 \to 0$ the maximum dissipated energy from (37) tends to the same value given in (24) and when $\omega_n/\omega_0 \to 1$ the maximum dissipated energy tends to zero. The maximum energy dissipation increases as the frequency ratio decreases.

However, the value of the threshold friction force must be computed to check whether the optimum predicted by Eq. (35) can occur in the continuous sliding range. At the onset of continuous sliding motion both conditions (30) and (31) hold and the following expression for $f_r|_{threshold}$ can be obtained:

$$f_r|_{threshold} = B\left(\frac{\omega_n}{\omega_0}, \xi\right) \Big/ \sqrt{1 + C\left(\frac{\omega_n}{\omega_0}, \xi\right)^2}. \tag{38}$$

The expression for C is given in Appendix B. In Fig. 7 curves of the ratio between the threshold friction force and the friction force computed from the value of $\omega_0 t_1|_{\max}$ given by (35), versus the frequency ratio, are shown for several values of ξ. Note that the force ratio does not increase continuously but goes through a maximum as ξ increases.

It can be concluded that for $\omega_n/\omega_0 < 1$ and $0 < \xi < 0.5$ the threshold friction force is always greater than the optimum friction force predicted by (35) and that the maximum energy dissipation occurs in the continuous sliding motion range. However, for damping ratios above 0.5 there is a range of frequency ratios where the threshold friction force is lower than the optimum. This means that this optimum is not really such because for that value of the friction force the system is still in the stick-slip region. Therefore, the optimum friction force and the maximum energy dissipation have to be determined numerically for the range of damping and frequency

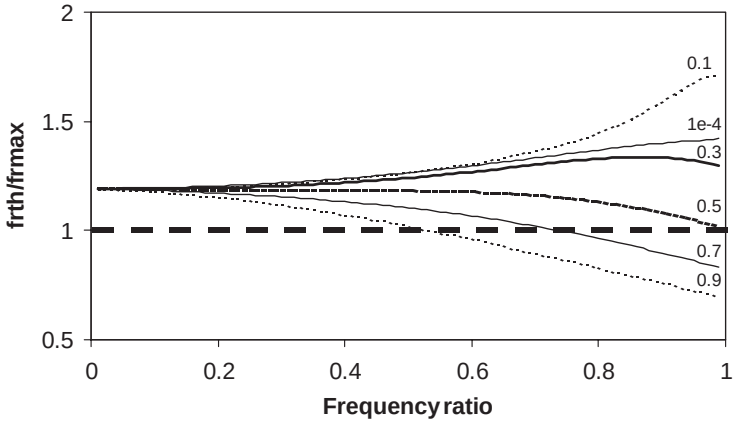

Fig. 7. Ratio of the threshold friction force to the friction force for maximum energy dissipation for several damping ratios.

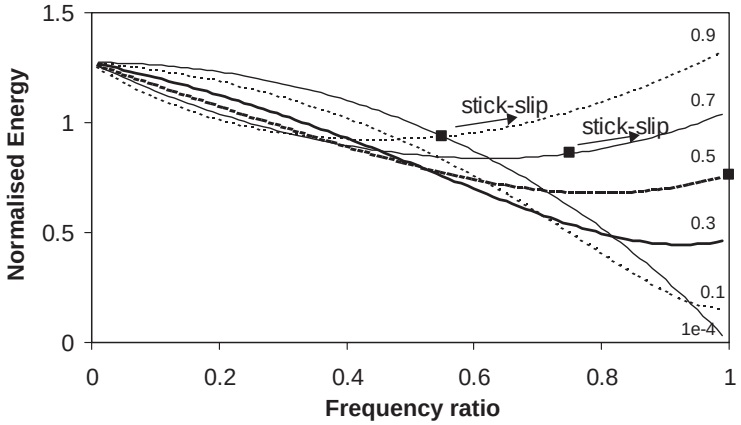

Fig. 8. Maximum dissipated energy versus frequency ratio for several values of the damping ratio.

ratios under the identity line in Fig. 7. For the rest of damping and frequency values the maximum dissipated energy has been computed by substituting Eq. (35) into (34) and the curves shown in Fig. 8 have been obtained. The squares on the curves corresponding to the damping ratios 0.7 and 0.9 indicate the beginning of the numerically computed values. In that region the maximum energy dissipation occurs in the stick-slip regime.

The first comment that can be made is that as $\omega_n/\omega_0 \to 0$ and $\xi \to 0$ the maximum dissipated energy tends to the value given by (24). For damping ratios below approximately 0.2, the maximum energy dissipation increases as the frequency ratio decreases. However, for higher damping ratios the dissipated energy curve goes through a minimum as the frequency ratio decreases and for damping ratios above approximately 0.8 the maximum energy dissipation is higher for $\omega_n/\omega_0 \cong 1$ than for $\omega_n/\omega_0 \cong 0$.

For frequency ratios below approximately 0.3 the maximum energy dissipation increases as the damping ratio decreases, but for frequency ratios close to 1 the opposite is true and the energy dissipation increases as the damping ratio increases. For $0.3 < \omega_n/\omega_0 < 1$ the maximum dissipated energy goes through a minimum as the damping ratio increases.

In light of the above results it can be concluded that choosing the natural frequency of the friction damper well below the vibration frequency of the main structure and making the damping as low as possible will give the maximum energy dissipation. A design with a frequency ratio close to one and a damping ratio above 50% is difficult to achieve in practice.

5. Conclusions and comments

In the above presented work simple analytical models have been used to study the behaviour of a ring damper. The general trends to follow in order to maximize energy dissipation have been established and are summarized now:

- The optimum value of the friction force that maximizes energy dissipation is constant for a given vibration amplitude of the driving system and a given mass of the damper.

- For a small damper mass relative to the mass of the driving system the dissipated energy is proportional to the damper mass.
- The natural frequency of the damper should be low compared to the oscillation frequency of the main system.
- The internal damping of the damper should be low. This explains why a steel ring, which has a very low internal damping, is a very effective friction damper.

The same trends identified in this work have been found in laboratory measurements with ring damped wheels [14,15].

Acknowledgements

The first author was supported by CEIT (Centro de Estudios e Investigaciones Técnicas) in San Sebastian (Spain) during the first part of this research work.

Appendix A. A different model for the friction force

In this work the vibrations of a mass on a moving base (Fig. 2) driven by the friction force between them have been analyzed using the conventional Coulomb friction law (Fig. 1(a)). In the following derivations the consequences of having different static and dynamic friction coefficients (Fig. 1(b)) will be investigated.

Once a steady state is reached, Eq. (20), which gives the normalized energy as a function of the normalized friction force and the time instants t_1 and t_2, is still valid. But the regions where stick-slip or continuous sliding occur and the corresponding values for t_1 and t_2, have to be determined again.

Now define a static and a dynamic normalized friction force:

$$\frac{\mu_s N}{\omega_0^2 X_0 m} = f_s, \quad \frac{\mu_d N}{\omega_0^2 X_0 m} = f_d, \quad \gamma = \frac{f_d}{f_s} = \frac{\mu_d}{\mu_s}. \tag{A.1}$$

Case 1: Stick-slip. In this region Eqs. (2) and (4) become (A.2) and (A.3), respectively:

$$\sin \omega_0 t_1 = f_s, \tag{A.2}$$

$$\omega_0 \gamma f_s (t_2 - t_1) = \cos \omega_0 t_1 - \cos \omega_0 t_2. \tag{A.3}$$

The stick-slip region, if it exists, will occur for a certain range of values of the static friction force: $1 > f_s > f_{s_1}$. The limiting value corresponds to the moment when the mass times the base acceleration at time t_2 equals de dynamic friction force:

$$\sin \omega_0 t_2 = -\gamma f_{s_1}. \tag{A.4}$$

From (A.2) to (A.4) and taking into account that $\omega_0 t_2 > \pi$, an expression for the limiting value of the static friction force can be obtained:

$$\gamma f_{s_1}(\pi + \sin^{-1}(\gamma f_{s_1}) - \sin^{-1}(f_{s_1})) = \sqrt{1 - f_{s_1}^2} + \sqrt{1 - \gamma^2 f_{s_1}^2}. \tag{A.5}$$

The existence of the stick-slip region depends on the ratio of the dynamic friction force to the static friction force, γ. Making $f_{s_1} = 1$ in Eq. (A.5) and expression for the minimum value of γ for which a stick-slip region exists can be found.

$$\left(\frac{\pi}{2} + \theta\right) \tan\theta = 1 \quad \text{with} \quad \gamma = \sin\theta. \tag{A.6}$$

This equation can be numerically solved to obtain $\gamma \cong 0.44$. If the ratio of dynamic to static friction force is higher than 0.44 a stick-slip region will exist.

Case 2: Continuous sliding. In this case, Eq. (A.3) still holds and also that $\omega_0 t_2 = \omega_0 t_1 + \pi$. The normalized energy dissipation can be calculated using Eq. (22) with the dynamic friction force as friction force. The continuous sliding region corresponds to a certain range of values of the static friction force: $0 < f_s < f_{s_2}$. The limiting value corresponds to the moment when the mass times the base acceleration at time t_2 equals the static friction force:

$$\sin\omega_0 t_2 = -f_{s_2}. \tag{A.7}$$

Combining (A.3), (A.7) and the periodicity relationship the following expression can be derived:

$$f_{s_2} = \sqrt{\frac{1}{1 + \dfrac{\pi^2\gamma^2}{4}}}. \tag{A.8}$$

Substituting the above expression in Eq. (22) the normalized energy dissipation at the beginning of the continuous sliding region can be obtained.

$$e_d|_{f_{s_2}} = \frac{4\gamma}{1 + \dfrac{\pi^2\gamma^2}{4}}. \tag{A.9}$$

Case 3: ''Uncertain'' region. The question now is the following: what happens in the region $f_{s_1} > f_s > f_{s_2}$? For this range of values of the static friction force, the mass times the acceleration of the base at time t_2 is higher than the dynamic friction force and lower than the static friction force. Therefore both the stick-slip and the continuous sliding regimes are possible. It is out of the scope of this work to investigate the conditions that would lead to one or the other behaviour of the system. Instead, the consequences of this uncertainty for the conditions of maximum energy dissipation will be analysed.

In Fig. 9 the normalized energy dissipation as a function of the normalized static friction force is shown for two different values of γ. In the ''uncertain'' region two different curves can be seen. The upper curve corresponds to the continuous sliding regime and the lower to the stick-slip regime.

In the situation shown in the upper graph ($\gamma = 0.7$) the maximum energy dissipation occurs in the region of continuous sliding and, therefore, the conclusions derived in Section 2 are valid. However, for $\gamma = 0.5$ the maximum of the energy dissipation curve for continuous sliding occurs

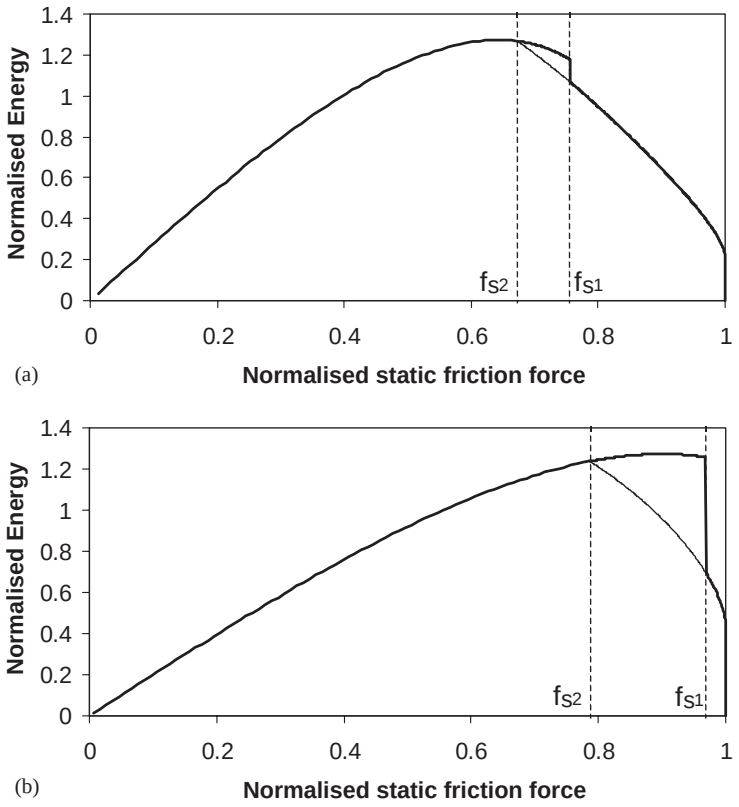

Fig. 9. Dissipated energy versus static friction force. (a) $\gamma = 0.7$ and (b) $\gamma = 0.5$.

in the "uncertain" region. If the system chooses for the continuous sliding regime, then the maximum energy dissipation will still be given by (24). But if the system stays in the stick-slip regime, the maximum normalized energy dissipation will occur when $f_s = f_{s_2}$ and its expression is given in (A.9). In that case, the maximum normalized energy dissipation is no longer constant and is a function of γ.

The last step is to determine the limiting value of γ above which the maximum energy dissipation occurs in the continuous sliding region and, thus, above which the results of the analysis carried out in Section 2 are valid. The limiting case is such that the normalized dynamic friction for maximum energy dissipation, Eq. (23), equals f_{s_2}. Combining (23) and (A.8):

$$\gamma_{\min} = \frac{2}{\pi} \cong 0.64. \tag{A.10}$$

In the case of ring dampers for railway wheels dry contact between two steel surfaces occurs and $\gamma \cong 0.7$. Therefore, it can be concluded that the analysis based on the classical Coulomb friction law presented in Section 2 leads to acceptable conclusions.

Appendix B. Stability of the periodic oscillations

The explicit form of Eq. (10) for the system in Fig. 2(b) is

$$\dot{\mathbf{x}}(t) = \mathbf{A}(t)\mathbf{x}(t) + \mathbf{b}(t) \quad \text{with } \mathbf{x}(t)^{\mathrm{T}} = [x(t) \quad \dot{x}(t)] \tag{B.1}$$

$$\text{stick phase}: \mathbf{A} = \begin{bmatrix} 0 & 1 \\ 0 & 0 \end{bmatrix}, \quad \mathbf{b} = \begin{bmatrix} 0 \\ \ddot{x}_0(t) \end{bmatrix},$$

$$\text{slip phase}: \mathbf{A} = \begin{bmatrix} 0 & 1 \\ -\omega_n & -2\xi\omega_n \end{bmatrix}, \quad \mathbf{b} = \begin{bmatrix} 0 \\ \pm \dfrac{F_r}{m} \end{bmatrix}.$$

Since the system is piecewise linear, the fundamental solution matrix for a time interval D in which the system is slipping, can be written as

$$\mathbf{\Phi}(t) = \mathrm{e}^{\mathbf{A}t}, \quad t \in D. \tag{B.2}$$

As explained in Section 2.2 a discontinuity occurs when the block changes from the slip to the stick phase, for the stick-slip periodic solution, or when the acceleration of the block changes sign, for the continuous sliding solution. This discontinuity is accounted for by introducing saltation matrices in the calculation of the monodromy matrix. The saltation matrix for a non-linear non-autonomous system is given by [13]

$$\mathbf{S} = \mathbf{I} + \frac{(\mathbf{f}_{\mathbf{p}+} - \mathbf{f}_{\mathbf{p}-})\mathbf{n}^{\mathrm{T}}}{\mathbf{n}^{\mathrm{T}}\mathbf{f}_{\mathbf{p}-} + \dfrac{\partial h}{\partial t}(t_p, \mathbf{x}(t_p))}, \tag{B.3}$$

where $\mathbf{f}_{\mathbf{p}-}$ and $\mathbf{f}_{\mathbf{p}+}$ are the value of the function left and right of the discontinuity point, $h(t, \mathbf{x})$ is a scalar function that defines the switching boundary and, $\mathbf{n} = grad(h(t, \mathbf{x}))$ is the vector normal to this line. For the system discussed here, the switching boundary function and its derivative and gradient take the following values:

$$h(t, \mathbf{x}) = \dot{x}_2 - \dot{x}_0(t), \quad \frac{\partial h}{\partial t}(t, \mathbf{x}) = -\ddot{x}_0(t), \quad \mathbf{n}_{\mathbf{p}} = \begin{bmatrix} 0 \\ 1 \end{bmatrix}. \tag{B.4}$$

B.1. Stability of the stick-slip periodic solution

It has already been explained in Section 2.2 that for the stick-slip periodic solution a discontinuity occurs when the block changes from the slip to the stick phase. For the friction law chosen (Fig. 1(a)), the change from stick to slip is smooth and the saltation matrix is equal to the identity matrix. At the point of change from slip to stick the left and right side values of the function describing the system are

$$\mathbf{f}_{\mathbf{p}-} = \begin{bmatrix} \dot{x}_0(t_p) \\ \omega_0^2 X_0 f_r - \omega_n^2 x_2(t_p) - 2\xi\omega_n \dot{x}_2(t_p) \end{bmatrix}, \quad \mathbf{f}_{\mathbf{p}+} = \begin{bmatrix} \dot{x}_0(t_p) \\ \ddot{x}_0(t_p) \end{bmatrix}. \tag{B.5}$$

The above expressions, together with (B.4) can be substituted in Eq. (B.3) to obtain the saltation matrix $\mathbf{S}_1$ from Eq. (13). That $\mathbf{S}_1$ is singular implies that one of the Floquet

multipliers will always be zero. The implications of this result have already been discussed in Section 2.2.

For the example in Fig. 2(a) ($\omega_n = 0, \xi = 0$), the fundamental solution matrices for the stick and for the slip phase are the same:

$$\mathbf{\Phi}(\Delta t_i) = \mathbf{\Phi}^S(\Delta t_i) = \mathrm{e}^{\mathbf{A}}\Delta t_i = \begin{bmatrix} 1 & \Delta t_i \\ 0 & 1 \end{bmatrix}. \tag{B.6}$$

If Eqs. (13) and (B.6) are introduced in (12), the monodromy matrix given in (14) can be obtained. The corresponding Floquet multipliers are 1 and 0. In this case, the eigenvalue 1 is related to a "rigid body" motion of the block. If the block is lifted and placed at another position, it will stay there. The eigenvalue 0 is related to the velocity of the block and it means that the velocity of the block will converge to its stable value within a cycle of the motion. Therefore, it can be said that the solution is stable.

If a spring is attached to the mass, but the damping is kept to zero, the fundamental solution matrix for the stick phase is still given by (B.6), but the fundamental solution matrix for the slip phase can be written as follows:

$$\mathbf{\Phi}(\Delta t_i) = \begin{bmatrix} \cos \omega_n \Delta t_i & \dfrac{1}{\omega_n} \sin \omega_n \Delta t_i \\ -\omega_n \sin \omega_n \Delta t_i & \cos \omega_n \Delta t_i \end{bmatrix}. \tag{B.7}$$

The time instants when the mass changes from stick to slip and back can be determined from Eqs. (26)–(30) with $\xi = 0$. If Eqs. (13), (B.6) and (B.7) are substituted in (12), an expression for the monodromy matrix can be derived:

$$\mathbf{\Phi_T} = \begin{bmatrix} \cos \omega_n \Delta t_5 \, cos \, \omega_n \Delta t_3 \cos \omega_n \Delta t_1 & \dfrac{1}{\omega_n} \cos \omega_n \Delta t_5 \cos \omega_n \Delta t_3 \sin \omega_n \Delta t_1 \\ -\omega_n \sin \omega_n \Delta t_5 \cos \omega_n \, \Delta t_3 \cos \omega_n \Delta t_1 & -\sin \omega_n \Delta t_5 \cos \omega_n \Delta t_3 \sin \omega_n \Delta t_1 \end{bmatrix}. \tag{B.8}$$

This matrix has the following eigenvalues:

$$\begin{aligned} &\lambda_1 = \cos^2 \omega_n \Delta t_3 < 1 \quad (\Delta t_3 = \Delta t_5 + \Delta t_1), \\ &\lambda_2 = 0. \end{aligned} \tag{B.9}$$

Since it is known from Section 2 that $0 < \Delta t_3 \leqslant \pi/\omega_0$ and $0 < \omega_n/\omega_0 < 1$, it is clear from the above that the Floquet multipliers are always smaller than one and that the system is stable.

B.2. Stability of the continuous sliding periodic solution

In the continuous sliding regime, the acceleration of the block changes sign every time the velocity of the block equals the velocity of the base and a jump occurs. The functions describing

the motion of the system left and right of the discontinuity point are

$$\mathbf{f}_{\mathbf{p}-} = \begin{bmatrix} \dot{x}_0(t_p) \\ \omega_0^2 X_0 f_r - \omega_n^2 x_2(t_p) - 2\xi\omega_n \dot{x}_2(t_p) \end{bmatrix},$$

$$\mathbf{f}_{\mathbf{p}+} = \begin{bmatrix} \dot{x}_0(t_p) \\ -\omega_0^2 X_0 f_r - \omega_n^2 x_2(t_p) - 2\xi\omega_n \dot{x}_2(t_p) \end{bmatrix}. \tag{B.10}$$

The above expressions correspond to a change from positive to negative acceleration, but the same result is obtained for the change from negative to positive acceleration. The time instant t_p can be obtained from (32). If the expressions (B.10) and (B.4) are introduced in (B.3) the saltation matrix, $\mathbf{S}$ from equation (15), can be obtained:

$$\mathbf{S} = \begin{bmatrix} 1 & 0 \\ 0 & 1 - \dfrac{2}{1 + \dfrac{\sin\omega_0 t_p}{f_r} - \dfrac{\omega_n^2}{\omega_0^2}\dfrac{x_2(t_p)}{X_0 f_r} - 2\xi\dfrac{\omega_n}{\omega_0}\dfrac{\cos\omega_0 t_p}{f_r}} \end{bmatrix}. \tag{B.11}$$

In order to be able to establish the magnitude of the second term of the diagonal of $\mathbf{S}$, Eqs. (32) and (38) from Section 4 will be used:

$$f_r = B\left(\frac{\omega_n}{\omega_0}, \xi\right)\cos\omega_0 t_p \quad \text{with } B\left(\frac{\omega_n}{\omega_0}, \xi\right) = \frac{1}{2}\frac{\omega_d}{\omega_0}\frac{\left(e^{\xi\omega_n\pi/\omega_0} + e^{-\xi\,\omega_n\pi/\omega_0} + 2\cos\dfrac{\omega_d\pi}{\omega_0}\right)}{\sin\dfrac{\omega_d\pi}{\omega_0}}, \tag{B.12}$$

$$f_r|_{threshold} = f_{r_{th}} = B\left(\frac{\omega_n}{\omega_0}, \xi\right) \Big/ \sqrt{1 + C\left(\frac{\omega_n}{\omega_0}, \xi\right)^2}$$

$$\text{with } C\left(\frac{\omega_n}{\omega_0}, \xi\right) = \frac{\omega_d}{\omega_0}\frac{\left(e^{\xi\omega_n\pi/\omega_0} + \cos\dfrac{\omega_d\pi}{\omega_0} + \dfrac{\xi}{\sqrt{1-\xi^2}}\sin\dfrac{\omega_d\pi}{\omega_0}\right)}{\sin\dfrac{\omega_d\pi}{\omega_0}}. \tag{B.13}$$

If Eqs. (28), (B.12) and (B.13) are introduced in (B.11) a new expression for the saltation matrix can be obtained.

$$\mathbf{S} = \begin{bmatrix} 1 & 0 \\ 0 & 1 - \dfrac{2}{2 + \sqrt{\dfrac{1}{f_r^2} - \dfrac{1}{B^2}} - \sqrt{\dfrac{1}{f_{r_{th}}^2} - \dfrac{1}{B^2}}} \end{bmatrix}. \tag{B.14}$$

From (B.13) it is clear that $f_{r_{th}} < B$ and from the definition of the threshold friction force, $f_r < f_{r_{th}}$, which leads to the conclusion that $0 < S_{22} < 1$ for all values of f_r, $\omega_n/\omega_0 < 1$ and ξ.

From the above and from the analysis in Eq. (18) it can be concluded that the determinant of the monodromy matrix is always smaller than 1. But that does not guarantee that both eigenvalues will be smaller than one. In order to check that the Floquet multipliers are smaller

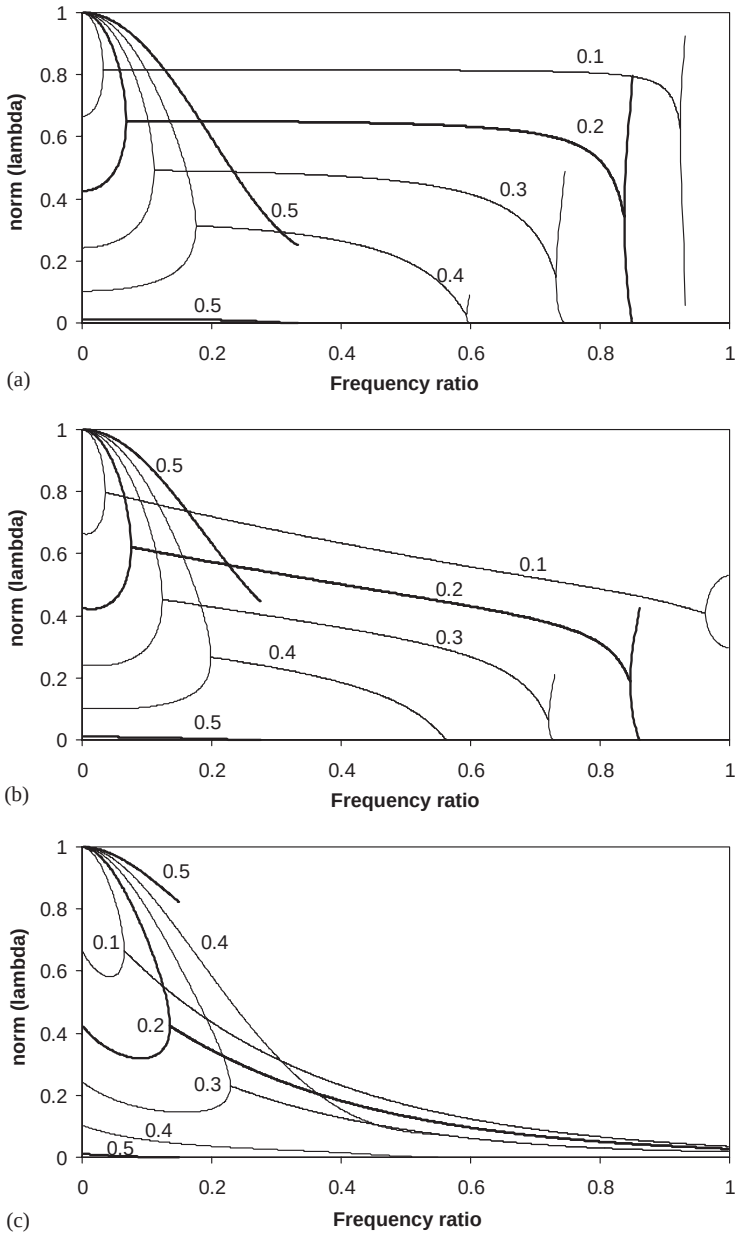

Fig. 10. Norm of the Floquet multipliers versus frequency ratio. (a) $\xi = 0$, (b) $\xi = 0.1$ and (c) $\xi = 0.5$.

than 1, the eigenvalues of the monodromy matrix in Eq. (15) have been numerically calculated using also (B.2), (B.12), (B.13) and (B.14). In Fig. 10 the Floquet multipliers are plotted as a function of ω_n/ω_0 for several values of the non-dimensional friction coefficient and three different values of the damping ratio.

The norm of the Floquet multipliers is smaller than 1 for all cases, which means that the continuous sliding periodic solution is stable in the range of frequency ratios and damping ratios studied.

For $\omega_n/\omega_0 \to 0$ the Floquet multipliers are real and tend to the values given in (17), regardless of the value of the damping ratio. As the frequency ratio increases the Floquet multipliers can become a pair of complex conjugate values and as the frequency increases further they become real again. The curves stop at the frequency ratio where the motion changes from continuous sliding to stick-slip for that value of the non-dimensional frequency parameter. For the case with no damping, Fig. 10(a), the Floquet multipliers tend to the values given in Eq. (B.9) as the frequency ratio approaches the threshold value. If damping is included, the Floquet multipliers at the threshold frequency are smaller than the values obtained with no damping. Therefore, the stick-slip periodic solution is also stable when damping is included.

References

[1] J.P. Den Hartog, Forced vibrations with combined Coulomb and viscous friction, *Transactions of the American Society of Mechanical Engineers* 53 (1931) 107–115.

[2] E.S. Levitan, Forced oscillation of a spring-mass system having combined Coulomb and viscous damping, *Transactions of the American Society of Mechanical Engineers* 32 (1960) 1265–1269.

[3] M.S. Hundal, Response of a base excited system with Coulomb and viscous friction, *Journal of Sound and Vibration* 64 (1979) 371–378.

[4] T.K. Pratt, R. Williams, Nonlinear analysis of stick/slip motion, *Journal of Sound and Vibration* 74 (1981) 531–542.

[5] C.F. Beards, J.L. Williams, The damping of structural vibration by rotational slip in joints, *Journal of Sound and Vibration* 53 (1977) 333–340.

[6] C.F. Beards, A. Woowat, The control of frame vibration by friction damping in joints, *ASME Vibration, Acoustic Stress and Reliability in Design* 107 (1985) 27–32.

[7] R.A. Ibrahim, Friction-induced vibration, chatter, squeal, and chaos Part II: Dynamics and modeling, *Applied Mechanics Review* 47 (7) (1994) 227–253.

[8] A. Akay, Acoustics of friction, *Journal of the Acoustical Society of America* 11 (4) (2002) 1525–1548.

[9] I. López, Theoretical and Experimental Analysis of Ring-damped Wheels, Ph.D. Thesis, University of Navarra, 1999.

[10] M.A. Heckl, Curve squeal of train wheels: unstable modes and limit cycles, *Proceedings of the Royal Society London* 458 (2002) 1949–1965.

[11] M.A. Heckl, I.D. Abrahams, Curve squeal of train wheels, Part 2: which wheel modes are prone to squeal?, *Journal of Sound and Vibration* 229 (3) (2000) 695–707.

[12] F. Krüger, E. Tassilly, D.J. Thompson, J.G. Walker, T. Ten Wolde, Lecture Notes on Railway Noise Control, COMETT program, 1993.

[13] R. Leine, Bifurcations in Discontinuous Mechanical Systems of Filippov type, Ph.D. Thesis, Technical University Eindhoven, 2000.

[14] I. López, A. Castañares, J.M. Busturia, J. Viñolas, Assessment of the efficiency of ring dampers for railway wheels, in: ISMA23, International Conference on Noise & Vibration Engineering, 1998, pp. 745–752.

[15] I. López, J. Viñolas, J. M. Busturia, A. Castañares, Efficiency of ring dampers for railway wheels: laboratory and track measurements, in: 6th International Congress on Sound and Vibration, 1999, pp. 2531–2538.

[16] K. Deimling, P. Szilagyi, Periodic solutions of dry-friction problems, Zeitschrift für Angewandte Mathematik und Physik 45 (1994) 53–60.

[17] K. Deimling, *Multivalued Differential Equations*, De Gruyter, Berlin, 1992.

[18] M. Nakai, M. Yokoi, Mechanism for squeal noise elimination on railway wheels with rings, in: Inter-Noise 95, 1995, pp. 151–154.

[19] T.S. Parker, L.O. Chua, *Practical Numerical Algorithms for Chaotic Systems*, Springer, New York, 1989.